

Vertex renormalization in weak decays of Cooper pairs and cooling compact stars

Armen Sedrakian¹, Herbert Müther¹, and Peter Schuck²

¹*Institute for Theoretical Physics, Tübingen University, D-72076 Tübingen, Germany*

²*Groupe de Physique Théorique, Institut de Physique Nucléaire, 91406 Orsay, France*

(Dated: May 9, 2019)

At temperatures below the critical temperature of superfluid phase transition baryonic matter emits neutrinos by breaking and recombination of Cooper pairs formed in the condensate. The strong interactions in the nuclear medium modify the weak interaction vertices and the associated neutrino loss rates. We study these modifications non-perturbatively by summing infinite series of particle-hole diagrams in the S -wave superfluid neutron matter. We argue that a consistent approach requires fulfillment of the dispersion relations for the polarization tensor, which insure the unitarity of the S -matrix. The pairing and particle-hole interactions in neutron matter are described in the framework of the BCS and Fermi-liquid theories derived from microscopic interactions. The neutrino loss rates in the vector channel are enhanced compared to the rates derived from free-space weak vertices in the temperature domain close to the critical temperature, T_c , but are suppressed by factors 5-10 for temperatures below $0.5 T_c$. The vertex corrected axial vector current emission is suppressed by the ratio of the baryon to the neutrino velocity squared.

I. INTRODUCTION

Pair-correlated baryonic matter in compact stars emits neutrinos via the weak neutral current processes of pair-breaking and recombination [1, 2, 3]

$$\{NN\} \rightarrow N + N + \nu_f + \bar{\nu}_f, \quad N + N \rightarrow \{NN\} + \nu_f + \bar{\nu}_f, \quad (1)$$

where $\{NN\}$ refers to a Cooper pair, $N+N$ to two quasiparticle excitations, ν_f and $\bar{\nu}_f$ to the neutrino and anti-neutrino of flavor f . The process (1) is limited to the temperature domain $T^* \leq T \leq T_c$, where T_c is the critical temperature of pairing phase transition and $T^* \sim 0.2 T_c$. At and above T_c this reaction cannot occur, since momentum and energy cannot be conserved simultaneously in a process $N \rightarrow N + \nu_f + \bar{\nu}_f$, i. e., an on-mass-shell fermion cannot produce bremsstrahlung (in the absence of external gauge fields). At asymptotically low temperatures, $T \leq T^*$, the rate of the process (1) is exponentially small since the number of excitations out of the condensate is suppressed as $\exp(-\Delta/T)$, where $\Delta(T)$ is the gap in the quasiparticle spectrum.

Cooling simulations of neutron stars revealed the efficiency of the processes (1) in refrigerating the baryonic interiors of a compact star from temperatures $T \leq T_c \sim 10^9$ K down to temperatures of the order of 10^8 K [4, 5, 6, 7]. The temperature domain above corresponds to the *neutrino cooling era* that spans the time domain $10^2 \leq t \leq 10^5$ years. The predicted surface temperatures of neutron stars during this and the following *photon cooling era* (where the star loses its thermal energy by emission of photons from the surface) are sensitive to the neutrino emission rates within this time-domain. Remarkably, the process (1) relates the cooling rate of a compact star to the microscopic physics of its interiors and is particularly sensitive to the density-temperature phase diagram of paired baryonic matter. Therefore, the measurements of the surface (photon) luminosities of neutron stars and their interpretation in

terms of cooling simulations have predictive power for analyzing the phase diagram and composition of baryonic matter [8, 9, 10, 11].

The rate of the process (1) was computed independently (and within alternative methods) in Refs. [1, 2] in the case where the pairing interaction is in the 1S_0 partial wave, i. e., nucleons are paired in a spin-0, isospin-1 state. In propagator language these rates correspond to the *one-loop* approximation to the polarization tensor of baryonic matter [2, 11]. The authors of Ref. [2] also estimated the corrections to the weak neutral current vertex due to the strong interactions to be $O(1)$ in strong coupling. The one-loop result is also available for the reaction (1) in the high-density regime, where the pairing interaction is in the 3P_2 partial wave, i. e., nucleons are paired in a spin-1, isospin-1 state [12]. In this density regime the charged baryons become superconducting in the 1S_0 partial wave, with similar implications for the neutrino rates as for (charge-neutral) neutrons at low densities [13, 14].

In this work we set up a formalism for computing the vertex corrections to weak reaction rates that arise due to the strong interactions in baryonic matter. We consider the case of neutron matter at subnuclear densities, which we describe within the Landau Fermi-liquid theory derived from microscopic interactions. At these densities neutron matter is characterized by an isotropic order parameter arising from the interaction in the 1S_0 partial wave channel; we solve the corresponding problem of pairing in the framework of the Bardeen-Cooper-Schrieffer (BCS) theory. In the non-relativistic limit, the vector and axial vector weak vertices are associated with scalar and spinor perturbations. Thus, the problem of the weak vertex renormalization reduces to a study of the effective three-point vertices that sum-up particle-hole irreducible ladders in superfluid matter in the scalar and spin channels. These resummations arise in the theories of superfluid Fermi-liquids that are based on the quasiparticle random phase approximation (QRPA); in the low-frequency, long-wave-length limit these theories

describe the collective modes of superfluids [15, 16, 17]. Note that in the present problem of neutrino radiation the high-frequency and long-wave length domain is relevant, since the pair breaking requires perturbations that are large enough to break a Cooper pair, while the finite momentum transfer contributions are suppressed as the even powers of the baryon Fermi-velocity over the speed of light (neutrino velocity).

The renormalization of the weak vertices leads to additional contributions to the neutrino loss rate compared to the one loop approximation, since the effective vertices are complex in general and a larger number of topologically non-equivalent polarization tensors are possible. We confirm the estimate of Ref. [2] that the vertex corrections are of the order of $O(1)$ in the strong coupling and do not change the one-loop results by many orders of magnitude. Nevertheless, the details of the temperature dependence of the neutrino loss rates are significantly affected by the vertex corrections; these changes are significant enough to affect the cooling rates of neutron stars quantitatively. Our results are in contrast to the recent claim in Ref. [18], that the vertex corrections in the vector channel reduce the rates computed at the one-loop level by many orders of magnitude; we shall return to this problem in Section IV.

The paper is organized as follows. Section II introduces the Green's functions formalism and computes, for the sake of illustration, the neutrino rates at one-loop. In Sec. III the modifications of the weak interaction vertices are computed by summing up particle-hole ladders in superfluid neutron matter. Section IV is devoted to the computation of the full polarization tensor that includes the vertex corrections derived in the preceding Section. Section V contains our conclusion. Some technical details are relegated to the Appendix.

II. S-WAVE PAIR-CONDENSATION IN NEUTRON MATTER

The neutron pair-condensate at subnuclear densities will be described in the framework of the Fermi-liquid theory, which assumes that the elementary degrees of freedom are quasiparticles with well defined momentum-energy relation and infinite life-time. The interactions between the quasiparticles are then described in terms of Landau parameters which depend on the momentum transfer (or scattering angle). Since the scattering angles involved are typically small, the momentum dependence of Landau parameters is further approximated by the leading and next-to-leading order terms in the expansion in Legendre polynomial with respect to the scattering angle. The problem of pairing in neutron matter will be solved below within the BCS approximation, where the anomalous self-energy (the gap function) is computed from the bare (realistic) interaction while the normal self-energy is computed within the decoupling approximation which ignores the effects of pair-

correlations on the single particle spectrum of quasiparticles. A number of factors such as the renormalization of the pairing interaction [19, 20, 21, 22, 23, 24, 25, 26], the wave-function renormalization [27, 28, 29, 30], the self-consistency among the normal and anomalous self-energies [28], affect the absolute value of the gap. The role of these factors has not been settled yet, and we shall employ below the standard BCS approach which has led to convergent and verifiable results for neutron matter (see the reviews [31, 32, 33]).

Since the baryonic component of stellar matter is in thermal equilibrium to a good approximation, we shall adopt the Matsubara Green's functions for the description of the neutron condensate and for the evaluation of the polarization tensor. In the case of 1S_0 pairing these are defined as (e. g. Ref. [34], pg. 120)

$$\hat{G}_{\alpha\alpha'}(\mathbf{p}, \tau) = -\delta_{\alpha\alpha'} \langle T_\tau a_{p\alpha}(\tau) a_{p\alpha'}^\dagger(0) \rangle, \quad (2)$$

$$\hat{F}_{\alpha\alpha'}(\mathbf{p}, \tau) = \delta_{\zeta\zeta'} \langle T_\tau a_{-p\downarrow}(\tau) a_{p\uparrow}(0) \rangle, \quad (3)$$

$$\hat{F}_{\alpha\alpha'}^\dagger(\mathbf{p}, \tau) = \delta_{\zeta\zeta'} \langle T_\tau a_{p\uparrow}^\dagger(\tau) a_{-p\downarrow}^\dagger(0) \rangle, \quad (4)$$

where α stands for spin $\sigma = \uparrow, \downarrow$ and isospin ζ , τ is the imaginary time, T_τ is the imaginary time ordering symbol, $a_{p\sigma}^\dagger(\tau)$ and $a_{p\sigma}(\tau)$ are the creation and destruction operators. In the momentum representation the propagators are given by

$$\hat{G}_{\alpha\alpha'}(ip_n, \mathbf{p}) = \delta_{\sigma\sigma'} \delta_{\zeta\zeta'} \left(\frac{u_p^2}{ip_n - \epsilon_p} + \frac{v_p^2}{ip_n + \epsilon_p} \right), \quad (5)$$

$$\hat{F}_{\alpha\alpha'}(ip_n, \mathbf{p}) = -i\sigma_y \delta_{\zeta\zeta'} u_p v_p \left(\frac{1}{ip_n - \epsilon_p} - \frac{1}{ip_n + \epsilon_p} \right), \quad (6)$$

and $F_{\alpha\alpha'}^\dagger(ip_n, \mathbf{p}) = F_{\alpha\alpha'}(ip_n, \mathbf{p})$, where $p_n = (2n + 1)\pi T$ is the fermionic Matsubara frequency, σ_y is the y -component of the Pauli-matrix, $u_p^2 = (1/2)(1 + \xi_p/\epsilon_p)$ and $v_p^2 = 1 - u_p^2$ are the Bogolyubov amplitudes and

$$\epsilon_p = \sqrt{\xi_p^2 + \Delta_p^2} \quad (7)$$

is the quasiparticle spectrum, where $\xi_p = p^2/2m + \text{Re}\Sigma(p) - \mu$ is the spectrum in the unpaired state with m and μ being the bare mass and chemical potential. Here $\Sigma(p)$ and $\Delta(p)$ are the normal and anomalous self-energies. For the later diagrammatic analysis we shall need the hole propagator which is given by

$$\begin{aligned} \hat{G}_{\alpha\alpha'}^\dagger(ip_n, \mathbf{p}) &= \hat{G}_{\alpha\alpha'}(-ip_n, -\mathbf{p}) \\ &= -\delta_{\sigma\sigma'} \delta_{\zeta\zeta'} \left(\frac{u_p^2}{ip_n + \epsilon_p} + \frac{v_p^2}{ip_n - \epsilon_p} \right). \end{aligned} \quad (8)$$

Since the quasiparticles are confined to the vicinity of the Fermi-surface a momentum expansion of the normal self-energy can be carried around the Fermi momentum,

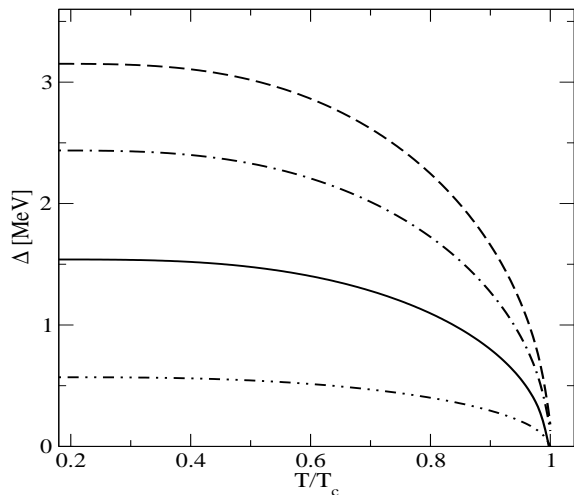


FIG. 1: Temperature dependence of the 1S_0 pairing gap in neutron matter for Fermi wave vectors $p_F = 0.4$ (solid line), 0.8 (dashed line), 1.2 (dashed-dotted line) and 1.6 (dashed-double-dotted line).

p_F , which leads to

$$\epsilon(p) = \frac{p_F}{m^*}(p - p_F) - \mu^*, \quad (9)$$

$$\frac{m^*}{m} = \left[1 + \frac{m}{p_F} \partial_p \text{Re}\Sigma(p) \Big|_{p=p_F} \right]^{-1}, \quad (10)$$

where $\mu^* \equiv -\epsilon(p_F) + \mu - \text{Re}\Sigma(p_F)$ is the effective chemical potential, m^* is the effective mass.

The off-mass-shell part of the self-energy will be approximated by its value on the mass shell; the wavefunction renormalization which accounts for the next-to-leading term in the expansion around the Fermi-energy is thus set to unity. The BCS mean-field approximation to the anomalous self-energy can be written in terms of the attractive four-point vertex function $\Gamma(p, p')$ in the form

$$\Delta(p) = -2 \int \frac{d^4 p'}{(2\pi)^4} \Gamma(p, p') \text{Im}F(p') f(\omega'), \quad (11)$$

where $f(\omega) = [1 + \exp(\beta\omega)]^{-1}$ is the Fermi distribution function and β is the inverse temperature. For the problem of neutron matter at subnuclear densities we adopt the standard BCS approach and thus approximate the four-point vertex by the bare interaction in the 1S_0 partial wave channel and the single particle spectrum by the on-shell spectrum given by Eq. (9). With these approximation Eq. (11) reduces to

$$\Delta(p) = \int \frac{d^3 p'}{2(2\pi)^3} V(p, p') \frac{\Delta(p')}{\sqrt{\xi(p')^2 + \Delta(p')^2}} [1 - 2f(\epsilon(p'))]. \quad (12)$$

The gap equation is supplemented by the equation for

TABLE I: Density dependence of the effective mass, the scalar and spin-spin interactions, the pairing gap and the critical temperature; the interactions are given in units of the density of states $\nu(p_F)$.

p_F [fm $^{-1}$]	m^*/m	v^V	v^A	$\Delta(p_F)$ [MeV]	T_c [MeV]
0.4	1.02	-0.56	0.55	1.54	0.85
0.6	1.00	-0.50	0.49	2.60	1.44
0.8	0.97	-0.47	0.44	3.15	1.78
1.0	0.94	-0.45	0.41	3.09	1.80
1.2	0.92	-0.43	0.40	2.44	1.46
1.4	0.88	-0.41	0.40	1.41	0.88
1.6	0.84	-0.36	0.39	0.57	0.38

the density of the system,

$$\rho = -2 \int \frac{d^4 p}{(2\pi)^4} \text{Im}G(p) f(\omega), \quad (13)$$

which determines the chemical potential in a self-consistent manner. Fig. 1 shows the temperature dependence of the 1S_0 pairing gap in neutron matter for several densities parameterized in terms of the Fermi wave number, $\rho = p_F^3/3\pi^2$. The gap at zero temperature and the critical temperature for unpairing are listed in the Table I.

Within the adopted Fermi-liquid description of neutron matter, the particle-hole interaction is given by

$$V^{ph}(\mathbf{q}) = v^V(\mathbf{q}) + v^A(\mathbf{q})(\boldsymbol{\sigma} \cdot \boldsymbol{\sigma}'), \quad (14)$$

where $\boldsymbol{\sigma}$ refers to the Pauli matrix. The Landau parameters $v^V(\mathbf{q})$ and $v^A(\mathbf{q})$ depend on the momentum transfer \mathbf{q} in the process where both fermion momenta are on the Fermi-surface (in the common notation these correspond to the f and g Landau parameters; the present notation anticipates that these constants are the driving terms in the vector and axial-vector channels). Note that the (small) tensor and spin-orbit terms are neglected in Eq. (14). The full dependence of these parameters on the momentum transfer is commonly approximated by a Legendre polynomial with respect to the angle formed by the incoming fermions, whereby only the leading and next-to-leading order terms contribute significantly.

Table I lists the effective mass, the zeroth order Landau parameters in the scalar and spin channels, and the pairing gap in the zero-temperature neutron matter computed with the CD Bonn potential [35]. The Landau parameters were computed by using the method of Ref. [36]. The solution of the gap equation was obtained by applying the iterative method with “running” cut-off as described in Ref. [37]. The values for pairing gaps quoted above should be viewed as an upper limit, since the wavefunction renormalization and the screening of pairing interaction are likely to reduce these values.

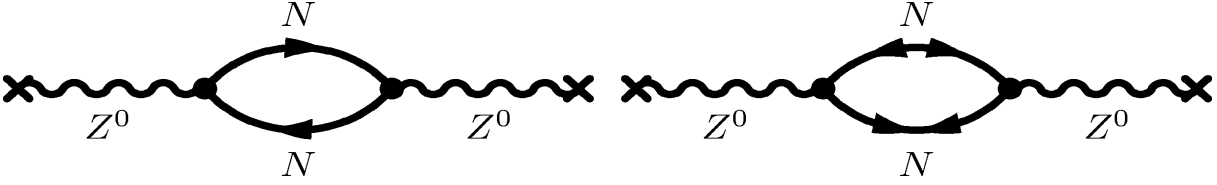


FIG. 2: The one-loop contribution to the polarization tensor in the superfluid matter; solid lines refer to the baryon propagators, wavy lines to the (amputated) Z^0 propagator.

III. THE PAIR-BREAKING PROCESSES AT ONE-LOOP

The neutrino emissivity (the power of the energy radiated per unit volume in neutrino-anti-neutrino pairs) is given by [2, 38]

$$\begin{aligned} \epsilon_{\nu\bar{\nu}} &= -2 \left(\frac{G}{2\sqrt{2}} \right)^2 \int \frac{d^3q_1}{(2\pi)^3 2\omega_1} \int \frac{d^3q_2}{(2\pi)^3 2\omega_2} \int dq_0 \\ &\times \int d^3\mathbf{q} \delta(\mathbf{q}_1 + \mathbf{q}_2 - \mathbf{q}) \delta(\omega_1 + \omega_2 - q_0) q_0 \\ &\times g(q_0) \Lambda^{\mu\zeta}(q_1, q_2) \Im \Pi_{\mu\zeta}(q), \end{aligned} \quad (15)$$

where G is the weak coupling constant, $q_i = (\omega_i, \mathbf{q}_i)$, $i = 1, 2$ are the on-mass-shell four-momenta of neutrinos, $g(q_0) = [\exp(q_0/T) - 1]^{-1}$ is the Bose distribution function, $\Pi_{\mu\zeta}(q)$ is the retarded polarization tensor,

$\Lambda^{\mu\lambda}(q_1, q_2) = \text{Tr} [\gamma^\mu (1 - \gamma^5) \not{q}_1 \gamma^\nu (1 - \gamma^5) \not{q}_2]$. Here and below the emissivities are given per neutrino flavor; the total rate is obtained upon multiplying the single flavor rate by the number of neutrino flavors within the standard model, $N_f = 3$. The polarization tensor of baryons at one-loop is shown in Fig. 2 and is given analytically by

$$\Pi^{V/A}(q) = T \sum_{\sigma, p} [G(p)G(p+q) \mp F(p)F^\dagger(p+q)], \quad (16)$$

where $p = (ip_0, \mathbf{p})$. The upper/lower signs correspond to vector current (V) and axial vector current (A) couplings, $\hat{G}_{\alpha\alpha'}(ip_n, \mathbf{p}) = \delta_{\sigma\sigma'} \delta_{\zeta\zeta'} G(ip_n, \mathbf{p})$ and $\hat{F}_{\alpha\alpha'}(ip_n, \mathbf{p}) = -i\sigma_y \delta_{\zeta\zeta'} F(ip_n, \mathbf{p})$. In writing Eq. (16) we assumed that baryons carry the same isospin quantum number.

Performing the Matsubara sums (see the Appendix) we obtain

$$\begin{aligned} \Pi^{V/A}(q) &= \sum_{\sigma p} [f(\epsilon_p) - f(\epsilon_k)] \left(\frac{A_\mp}{iq + \epsilon_p - \epsilon_k} - \frac{B_\mp}{iq - \epsilon_p + \epsilon_k} \right) \\ &+ \sum_{\sigma p} [f(-\epsilon_p) - f(\epsilon_k)] \left(\frac{C_\mp}{iq - \epsilon_k - \epsilon_p} - \frac{D_\mp}{iq + \epsilon_p + \epsilon_k} \right), \end{aligned} \quad (17)$$

where $k = p + q$, $A_\mp = u_p^2 u_k^2 \mp h$, $B_\mp = v_p^2 v_k^2 \mp h$, $C_\mp = u_k^2 v_p^2 \pm h$, $D_\mp = u_p^2 v_k^2 \pm h$, $h = u_p u_k v_p v_k$. To obtain the rate of neutrino generation (15) we need the imaginary part of the polarization tensor which, after analytical continuation in Eq. (17), becomes [note that $f(-\epsilon_p) = 1 - f(\epsilon_p)$]

$$\begin{aligned} \Im \Pi^{V/A}(q) &= -\pi \sum_{\sigma p} [f(\epsilon_p) - f(\epsilon_k)] (A_\mp + B_\mp) \delta(\omega + \epsilon_p - \epsilon_k) \\ &- \pi \sum_{\sigma p} [f(-\epsilon_p) - f(\epsilon_k)] [C_\mp \delta(\omega - \epsilon_p - \epsilon_k) - D_\mp \delta(\omega + \epsilon_p + \epsilon_k)]. \end{aligned} \quad (18)$$

To obtain the first line we used the fact that the quasiparticle spectra are invariant under spatial reflections, i. e., $\epsilon(-\mathbf{p}) = \epsilon(\mathbf{p})$.

The first line in Eq. (18) corresponds to the process of scattering where a quasiparticle is promoted out of the condensate into an excited state, or inversely, an excitation merges with the condensate. The corresponding piece of the response function $\Im \Pi^{V/A}(q)$ vanishes for small momentum transfers. Indeed neutrino energies are

of the order of temperature which implies that their wave vectors $q \sim \omega_\nu/\hbar c \sim T/\hbar c \sim 1/197.3 \ll 1$. On the other hand the neutron wave vectors $p \sim p_F \sim 1 \text{ fm}^{-1}$. Upon expanding the argument of the delta-function with re-

spect to $|q|$ around the point $q = 0$ one finds

$$\omega - q \frac{\xi_p}{\epsilon_p} \frac{\partial \xi_{p+q}}{\partial q} \Big|_{q=0} - q \frac{\Delta_p}{\epsilon_p} \frac{\partial \Delta_{p+q}}{\partial q} \Big|_{q=0} = 0. \quad (19)$$

If we assume that $\Delta \neq \Delta(p)$ the third term on the l. h. side vanishes. It follows that $x \equiv (\mathbf{p} \cdot \mathbf{q})/pq = (\epsilon_p/\xi_p)(\omega/vq) \leq 1$, where v ($\sim v_F$) is the baryon (Fermi) velocity. For on mass-shell neutrinos $\omega = cq$ and the latter condition can not be satisfied, i. e. the scattering contribution can be neglected. We shall not evaluate the effects of non-locality in the momentum and frequency domain on the neutrino rates here, as it will require modeling of the momentum and frequency dependence of the gap function (for the S -wave interactions the momentum dependence is described, e. g., in Refs. [30, 39, 40, 41] and

the energy dependence in Refs. [27, 28, 29]). The second line in Eq. (20) describes the process of pair-breaking and recombination, i. e., excitation of pairs of quasiparticles out of the condensate, and inversely, restoration of a pair within the condensate. Since we are interested in the emission process we shall keep only the terms that do not vanish for $\omega > 0$; then, the pair-braking contribution is given by

$$\Im \Pi^{V/A}(q) = -\pi \sum_{\sigma \mathbf{p}} [f(-\epsilon_p) - f(\epsilon_k)] C_{\mp}. \quad (20)$$

This contribution to the polarization tensor can be evaluated analytically in the limit $\mathbf{q} \rightarrow 0$ and the case $\Delta \neq \Delta(p)$ and is given by

$$\Im \Pi^V(q) = -2\pi \nu(p_F) g(\omega)^{-1} f\left(\frac{\omega}{2}\right)^2 \left(\frac{\Delta^2}{\omega^2}\right) \frac{\omega}{\sqrt{\omega^2 - 4\Delta^2}} \theta(\omega - 2\Delta), \quad (21)$$

$$\Im \Pi^A(q) \simeq 0 + O\left(\frac{v_F^2}{c^2}\right), \quad (22)$$

where $\nu(p_F) = m^* p_F / 2\pi^2$ is the density of states ($\hbar = 1$) and θ is the Heaviside step function; the explicit form of the $O(v_F^2/c^2)$ contribution to the axial current response is given in Ref. [1]. Note the threshold behavior of the vector current response, which is finite for frequencies that are large compared to 2Δ - the energy needed to break a pair.

Upon substituting Eq. (21) in Eq. (15) and carrying out the phase-space integrals we obtain the emissivity per neutrino flavor [1, 2]

$$\epsilon_{\nu\bar{\nu}} = \frac{G^2 c_V^2}{240\pi^3} \nu(p_F) T^7 I_1(\zeta) \equiv \epsilon_0 I_1(\zeta), \quad (23)$$

where $\zeta = 2\Delta(T)/T$ and

$$I_1(\zeta) = \zeta^7 \int_0^\infty d\phi (\cosh \phi)^5 f\left(\frac{\zeta}{2} \cosh \phi\right)^2. \quad (24)$$

Note that the rate (23) scales as ζ^7 and, consequently, it is most sensitive to the magnitude of the pairing gap. Because of the substantial density dependence of the gap, the emissivity (23) varies strongly across the stellar interior, with important implications for the cooling of neutron stars [4, 5, 6, 7, 8, 9, 10, 11].

IV. WEAK INTERACTION VERTICES

Consider the weak vector and axial vector vertices in the nuclear medium featuring a condensate. Because the particle-hole interactions in the medium (which are represented by the Landau parameters in Table I) are not small, the vertex renormalization requires a summation of an infinite number of particle-hole loops. There are four topologically non-equivalent vertices in the superfluid state in general, but, as we shall see, the particle-hole symmetry reduces their number by one. Since neutrons pair in an isospin-1 state (neutron-proton pairing is unimportant for large asymmetries [42, 43]) we shall suppress the isospin indices. Further we shall keep the lowest order Landau parameters in their expansion in Legendre polynomials, since the next-to-leading order terms are suppressed by powers of v_F/c . Thus, the effective particle-hole interaction is given by

$$v = v^V + v^A(\boldsymbol{\sigma} \cdot \boldsymbol{\sigma}'). \quad (25)$$

The integral equation defining the effective weak vertices, which we write in an operator form, are given by

$$\hat{\Gamma}_1^a = \Gamma_0^a + v^a(G\Gamma_1^a G + \hat{F}\Gamma_3^a G + G\Gamma_2^a \hat{F} + \hat{F}\Gamma_4^a \hat{F}), \quad (26)$$

$$\hat{\Gamma}_2^a = v^a(G\Gamma_2^a G^\dagger + \hat{F}\Gamma_4^a G^\dagger + G\Gamma_1^a \hat{F} + \hat{F}\Gamma_3^a \hat{F}), \quad (27)$$

$$\hat{\Gamma}_3^a = v^a(G^\dagger\Gamma_3^a G + \hat{F}\Gamma_1^a G + G^\dagger\Gamma_4^a \hat{F} + \hat{F}\Gamma_2^a \hat{F}), \quad (28)$$

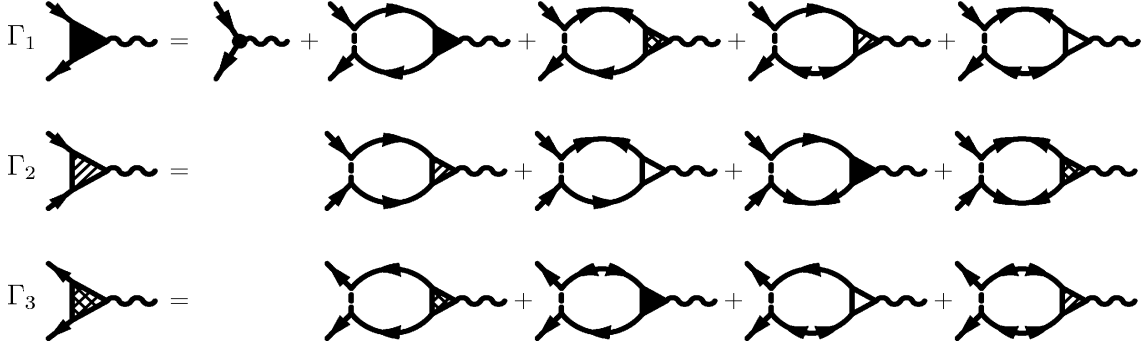


FIG. 3: Coupled integral equations for the effective weak vertices in superfluid baryonic matter. The “normal” Γ_1 vertex (full triangle) and two “anomalous” vertices Γ_2 (hatched) and Γ_3 (shaded triangle) are shown explicitly, the fourth vertex (empty triangle) is obtained by interchanging the particle and hole lines in the first line. The anomalous vertices vanish in the normal state.

and are displayed diagrammatically in Fig. 3. Here $\hat{F} = -i\sigma_y F$, v^a with $a \in V, A$ are defined in Eq. (25), while $\Gamma_0^V = 1$ and $\Gamma_0^A = \sigma$. The fourth integral equation for the vertex Γ_4^a follows upon interchanging in Eq. (26) particle and hole propagators $G \leftrightarrow G^\dagger$. The momentum space representation of Eq. (26) reads

$$\hat{\Gamma}_1^a(q) = \Gamma_0^a + v^a \int \frac{d^4 p}{(2\pi)^4} \left[G(p)\Gamma_1^a(q)G(p+q) + G(p)\Gamma_2^a(q)\hat{F}(p+q) \right. \\ \left. + \hat{F}(p)\Gamma_3^a(q)G(p+q) + \hat{F}(p)\Gamma_4^a(q)\hat{F}(p+q) \right], \quad (29)$$

with similar expressions for Eqs. (27) and (28). Even though the driving interactions are local in time, the resummations at finite temperatures lead to time-retarded interactions, which imply that the effective vertices in Eqs. (26)-(28) are complex in general. Considering the scalar interaction Γ_0^V we obtain

$$\begin{pmatrix} 1 - v^V[\Pi_{GG}(q) - \Pi_{FF}(q)] & \Pi_{GF}(q) & \Pi_{FG}(q) \\ -2\Pi_{GF}(q) & 1 - v^V\Pi_{GG^\dagger}(q) & \Pi_{FF}(q) \\ -2\Pi_{FG}(q) & \Pi_{FF}(q) & 1 - v^V\Pi_{G^\dagger G}(q) \end{pmatrix} \begin{pmatrix} \Gamma_1^V(q) \\ \Gamma_2^V(q) \\ \Gamma_3^V(q) \end{pmatrix} = \begin{pmatrix} \Gamma_0^V \\ 0 \\ 0 \end{pmatrix}, \quad (30)$$

where, using the abbreviations $X, X' \in G, F, G^\dagger$, we have (see the Appendix)

$$\Pi_{X, X'}(q) = \int \frac{d\omega}{2\pi} L_{X, X'}(q) = \int \frac{d^4 p}{(2\pi)^4} X(p)X'(p+q). \quad (31)$$

The loop integrals have the following symmetries: $L_{GG} = L_{G^\dagger G^\dagger}$, $L_{GF} = L_{FG^\dagger}$ and $L_{FG} = L_{G^\dagger F}$, which imply that $\Gamma_1^V = \Gamma_4^V$ and $\Gamma_1^A = -\Gamma_4^A$. For energy-momentum independent interactions the integral equation (30) reduces to three coupled linear equation for the complex functions Γ_i^V , $i = 1, 2, 3$. The details of the computation of the coefficients in Eqs. (30) are relegated to the Appendix. Fig. 4 shows the dependence of real and imaginary parts of the pair-breaking components of the polarization tensors in units of the density of states upon the frequency. The imaginary parts are odd while the real parts are even functions of the frequency. These are related by the Kramers-Kronig relation (A15), which follows from the unitarity of the S -matrix for the emission process of interest. The major contribution to the polarization tensor arises from the vicinity of the threshold $\omega = 2\Delta$; the asymptotic behavior of the Bogolyubov coefficient v_p guarantees that the polarization tensors vanishes for large frequencies. This is not the case for the polarization tensor $\Pi_{G^\dagger G}$. The correct asymptotics is obtained upon subtracting its counterpart in the normal state, since the resummation of the particle-hole ladders in the normal state have been already included in the definition of the vertex v^V . Thus, we consider below the quantity $\Pi_{G^\dagger G}(q, \Delta) - \Pi_{G^\dagger G}(q, 0)$. In the case of axial-vector interactions the effective vertices are given by

$$\begin{pmatrix} 1 & \Pi_{GF}(q) & \Pi_{FG}(q) \\ 0 & 1 - v^A\Pi_{GG^\dagger}(q) & \Pi_{FF}(q) \\ 0 & \Pi_{FF}(q) & 1 - v^A\Pi_{G^\dagger G}(q) \end{pmatrix} \begin{pmatrix} \Gamma_1^A(q) \\ \Gamma_2^A(q) \\ \Gamma_3^A(q) \end{pmatrix} = \begin{pmatrix} \Gamma_0^A \\ 0 \\ 0 \end{pmatrix}. \quad (32)$$

This equation has a “trivial” solution $\Gamma_1^A = 1$ and $\Gamma_2^A = \Gamma_3^A = 0$ to the leading order in the v_F^2/c^2 expansion.

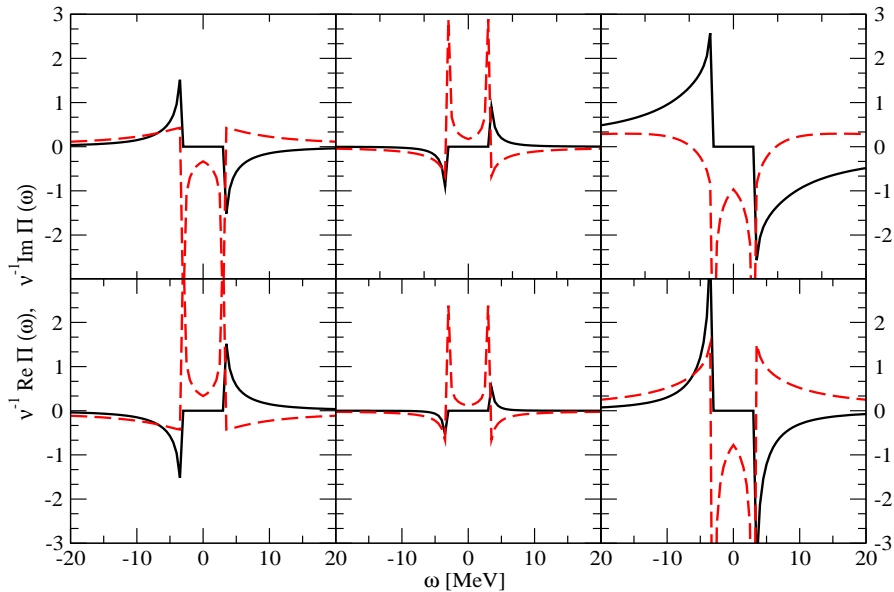


FIG. 4: (Color online) Dependence of the imaginary (solid) and real (dashed, red online) parts of the polarization tensors in units of density of states on the frequency for vanishing momentum transfer $\mathbf{q} = 0$. The density corresponds to $p_F = 1.2 \text{ fm}^{-1}$, the temperature $T/T_c = 0.85$. Upper panel from left to right: $\Pi_{GG}(\omega)$, $\Pi_{GF}(\omega)$, and $\Pi_{FG}(\omega)$; lower panel from left to right: $\Pi_{FF}(\omega)$, $\Pi_{GG^\dagger}(\omega)$ and $\Pi_{G^\dagger G}(\omega)$.

The dependence of the real and imaginary parts of the vector vertex functions on the frequency is shown in Fig. 5. The absolute magnitude of these vertices is representative for the magnitude of the suppression of the neutrino loss rates by the vertex corrections. Consistent with the properties of the polarization functions, the real parts are even, while the imaginary parts are odd with respect to the change in the sign of the frequency. At the frequency $\omega = 2\Delta$ the real and imaginary components of the vertices vanish, which guarantees the threshold behavior of the loss rates. At large frequencies ($\omega \rightarrow \infty$) one finds $\Gamma_1 \rightarrow v^V$ and $\Gamma_2 \sim \Gamma_3 \rightarrow 0$ asymptotically. Note that the “normal” vertex Γ_1 can not be approximated by its bare value at the frequencies $\omega \sim 2\Delta$ relevant for the loss processes; indeed, as seen in Fig. 5, its renormalization is substantial and it even changes its sign. The effective vertices are larger for temperatures closer to T_c , as seen from a comparison of the upper and lower panels in Fig. 5. As a result the neutrino loss rates are enhanced at $T \rightarrow T_c^-$.

In the relevant kinematical domain $2\Delta \leq \omega \leq \infty$ and $\mathbf{q} = 0$ the real components of vertices do not have poles, i. e., there are no collective excitations. The well-known *low-frequency, long-wave-length* collective modes of BCS superfluids are located in the domain $\omega \ll 2\Delta$. Their dispersion relation, corresponding to acoustic oscillations, is given by $\omega^2 = (v_F^2 q^2/3)[1 + \nu(p_F)v^V]$, to the leading order in v_F^2/c^2 expansion.

V. THE FULL POLARIZATION TENSOR AND THE EMISSIVITY

Having determined the effective vertices $\Gamma_i^V(\omega)$, we are in a position to construct the complete polarization tensor, which is given by the sum of diagrams in Fig. 6. The analytical form for the vector current contribution reads

$$\begin{aligned} \Pi^V(q) = \sum_{i=1}^3 \Pi_i^V(q) \Gamma_i^V(q) = T \sum_{\sigma,p} \left\{ [G(p)G(p+q) - F(p)F^\dagger(p+q)] \Gamma_1^V(\omega) \right. \\ \left. - G(p)F(p+q) \Gamma_2^V - F(p)G(p+q) \Gamma_3^V(\omega) \right\}. \end{aligned} \quad (33)$$

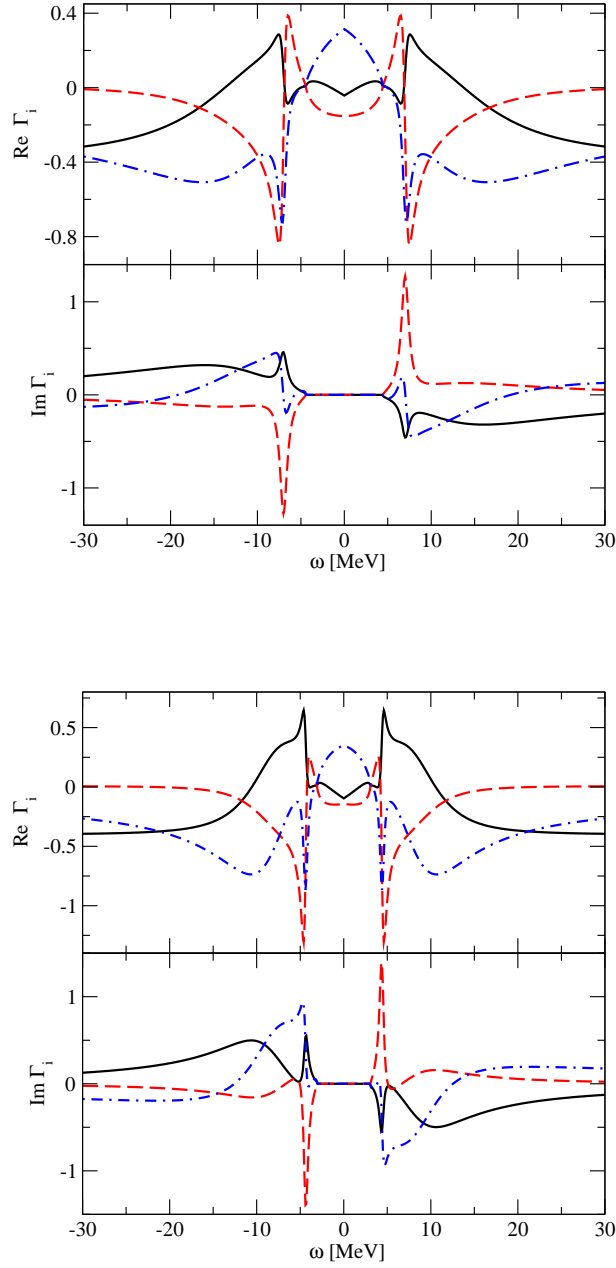


FIG. 5: (Color online) *Upper panel:* Dependence of the real (upper row) and imaginary (lower row) parts of the vertices Γ_i , $i = 1$ solid (black online) $i = 2$ dashed (red online) and $i = 3$ dashed-dotted (blue online) on the frequency for vanishing momentum transfer $\mathbf{q} = 0$. The density corresponds to $p_F = 1.2 \text{ fm}^{-1}$, the temperature $T/T_c = 0.6$. *Lower panel:* The same as in the upper panel, but for $T/T_c = 0.85$.

The analogous expression for the axial vector current contribution vanishes at the order we are working. We have seen in Sec. IV that the anomalous vertices $\Gamma_2^A = \Gamma_3^A = 0$; the remaining contribution

$$\Pi^A(q) = T \sum_{\sigma,p} \left\{ [G(p)G(p+q) + F(p)F^\dagger(p+q)] \Gamma_1^A(\omega) \right\}, \quad (34)$$

disappears because the expression in the brackets is $O(v_F^2/c^2)$, while $\Gamma_1^A(\omega) \sim O(1)$. The complete polarization tensor in the vector channel is shown in Fig. 7 for two temperatures $T/T_c = 0.6$ and $T/T_c = 0.85$ at $p_F = 1.2 \text{ fm}^{-1}$, along

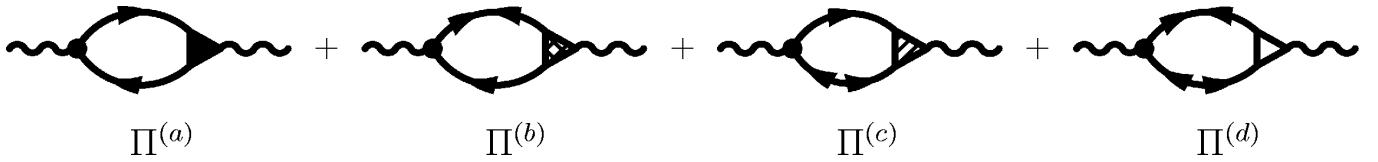


FIG. 6: The sum of polarization tensors that contribute to the neutrino emission rate. The contributions from $\Pi^{(b)}(q)$ and $\Pi^{(c)}(q)$ vanish at one-loop.

with the polarization tensor without vertex corrections. The full polarization tensor is reduced significantly (by a factor of 10) compared to its counterpart without vertex corrections. Apart from this main qualitative effect, finer modification include a redistribution of the weight from the threshold frequency in the one-loop case to the larger frequencies in multi-loop case and (related) broadening of the resonance structure in the latter case. Upon substituting Eq. (33) in Eq. (15) we obtain

$$\epsilon_{\nu\bar{\nu}} = \epsilon_0 (I_2 + I_3), \quad (35)$$

where

$$I_2 = -\frac{1}{\pi\nu(p_F)T^7} \int_0^\infty d\omega \omega^6 g(\omega) \sum_{i=1}^3 [\text{Im}\Pi_i(\omega) \text{Re}\Gamma_i(\omega)], \quad (36)$$

$$I_3 = -\frac{1}{\pi\nu(p_F)T^7} \int_0^\infty d\omega \omega^6 g(\omega) \sum_{i=1}^3 [\text{Re}\Pi_i(\omega) \text{Im}\Gamma_i(\omega)]. \quad (37)$$

These integrals are done numerically with the functions $\Pi_i(\omega)$ and $\Gamma_i(\omega)$ defined in the previous Section (see Figs. 4 and 5 therein). The integrals I_2 and I_3 are shown in Fig. 8 as a function of the reduced temperature T/T_c (lower

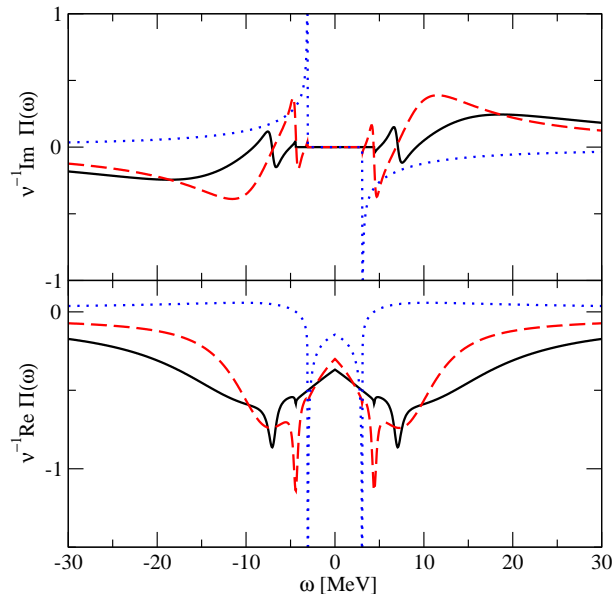


FIG. 7: (Color online) Dependence of the imaginary (upper panel) and real (lower panel) parts of the full vector current polarization tensor on the frequency at $p_F = 1.2 \text{ fm}^{-1}$ for $T/T_c = 0.6$ (solid line) and $T/T_c = 0.85$ (dashed line, red online). The polarization tensor without vertex corrections at $T/T_c = 0.85$ and reduced by factor 10, is shown by the dotted line (blue online).

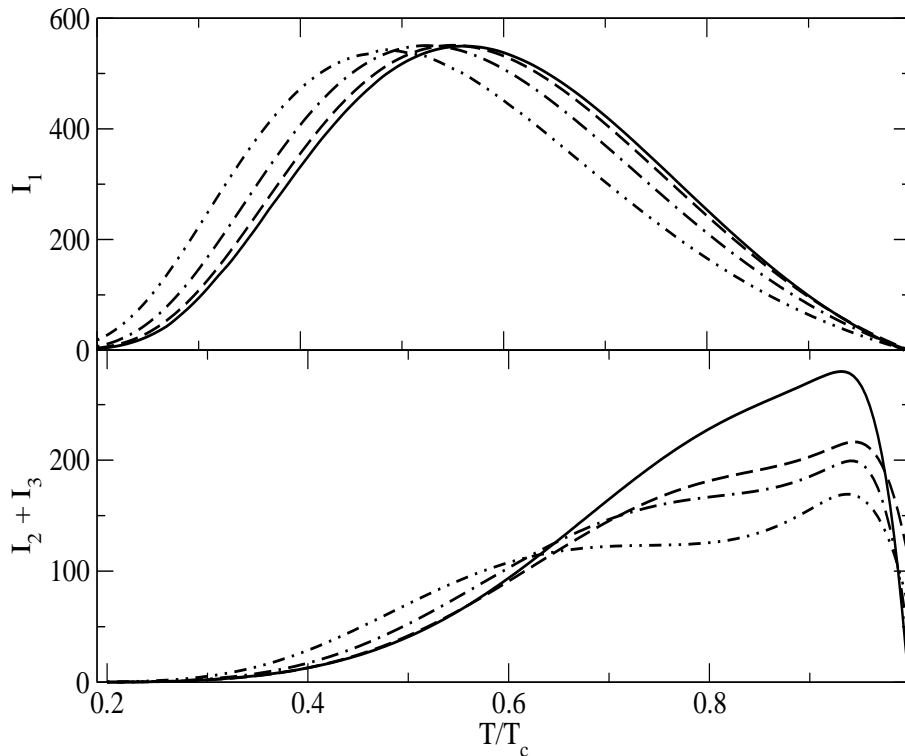


FIG. 8: Dependence of the integrals I_1 (upper panel) and I_2, I_3 (lower panel) on the reduced temperature for Fermi wave vectors $p_F = 0.4$ (solid line), 0.8 (dashed line), 1.2 (dashed-dotted line) and 1.6 (dashed-double-dotted line).

panel) along with the one-loop integral I_1 (upper panel). For $T \rightarrow T_c$ the both rates vanish, consistent with the observation that the pair bremsstrahlung is absent in normal matter for on-shell (non-interacting) baryons. At small $T \leq 0.3T_c$ the rates are suppressed exponentially as $\exp(-\Delta/T)$. The temperature domain intermediate between these limits is the most relevant for the neutrino losses via the pair-breaking process; within this domain the temperature dependence of the full and one-loop rates are substantial. The effect of vertex corrections is twofold: for temperatures $0.8 \leq T/T_c \leq 1$ the loss rate is moderately enhanced compared to the one-loop result; this can be traced back to the enhancement of the effective vertices in the domain $T \sim T_c^-$. At lower temperatures the rates are strongly suppressed; e. g. at $T/T_c = 0.6$ the vertex corrected rate is about 20% of the one-loop rate. Thus the one-loop rates provide the correct magnitude of the loss rates in the domain close to the critical temperature, but overestimate the true rate by large factors at lower temperatures. Note also that the density dependence of the full loss rate is stronger than in the one-loop case.

Our results are in contrast to those obtained in Ref. [18], where it was claimed that the vertex corrections suppress the one-loop rate by many orders of magnitude. One potential problem is that Ref. [18] employed vertices that are valid only in the low-frequency $\omega \ll 2\Delta$ and zero temperature limits - domains that are not relevant to the problem at hand. Furthermore, the vertices were assumed to be purely real, in which case the dispersion relations for the polarization tensor and the unitarity of the S -matrix are violated.

VI. SUMMARY

The neutrino loss rate from neutron superfluid at subnuclear densities via neutrino pair bremsstrahlung has been studied within a microscopic model based on the Fermi-liquid and BCS theories. The modifications of the weak interaction rates in the nuclear medium were studied by summing infinite series of irreducible particle-hole diagrams in terms of a contact (momentum and energy independent) driving interaction. These modifications are embodied in the vertex functions that are computed from polarization tensor components corresponding to the pair-breaking process within the kinematical domain $\omega \in [2\Delta; \infty]$ and $\mathbf{q} \rightarrow 0$. Special attention was paid to preserving the dispersion relations for the polarization tensor components, that are implied by the unitarity of the S -matrix for the emission process.

We find neutrino loss rates that are enhanced above their one-loop counterparts in the temperature domain close to the critical temperature, but are strongly reduced in the temperature domain below $0.5 T_c$. These findings are in qualitative agreement with the earlier estimate of these corrections in Ref. [2], but differ substantially at the quantitative level.

While we concentrated above on the neutral current interactions, our formalism can be adapted to compute the rates of charge-current Urca process $n \rightarrow p + e + \nu_e$ beyond the one-loop rate derived in Ref. [44]. These should be subject to strong correction due to the tensor neutron-proton correlations. Another aspect is the modification of rates from P -wave condensate in denser regions of neutron star cores; for that purpose the formalism above needs to be extended to the tensor 3P_2 - 3F_2 partial wave channel. Vertex corrections could be substantial in the related problem of neutrino emission and propagation in quark matter, where one-loop results for a number of processes became available recently [45, 46, 47, 48, 49, 50, 51, 52].

Acknowledgments

This work was, in part, supported by the Deutsche Forschungsgemeinschaft through the SFB 382.

APPENDIX A: LOOP INTEGRALS

Here we quote the results for the loop integrals and polarization tensors that have been used in the main text. The loop integrals are defined as products of the Matsubara Green's functions, after the Matsubara sums have been carried out (here $\mathbf{k} = \mathbf{p} + \mathbf{q}$)

$$\begin{aligned}
L_{GG}(q, \mathbf{p}) &= T \sum_{ip} G(ip, \mathbf{p}) G(ip + iq, \mathbf{k}) \\
&= \left\{ \frac{u_p^2 u_k^2}{iq + \epsilon_p - \epsilon_k} - \frac{v_p^2 v_k^2}{iq - \epsilon_p + \epsilon_k} \right\} [f(\epsilon_p) - f(\epsilon_k)] \\
&\quad + \left\{ \frac{u_k^2 v_p^2}{iq - \epsilon_p - \epsilon_k} - \frac{u_p^2 v_k^2}{iq + \epsilon_p + \epsilon_k} \right\} [f(-\epsilon_p) - f(\epsilon_k)], \tag{A1}
\end{aligned}$$

$$\begin{aligned}
L_{FG}(q, \mathbf{p}) &= T \sum_{ip} F(ip, \mathbf{p}) G(ip + iq, \mathbf{k}) \\
&= -u_p v_p \left[\frac{u_k^2}{iq + \epsilon_p - \epsilon_k} + \frac{v_k^2}{iq - \epsilon_p + \epsilon_k} \right] [f(\epsilon_p) - f(\epsilon_k)] \\
&\quad + u_p v_p \left[\frac{u_k^2}{iq - \epsilon_p - \epsilon_k} + \frac{v_k^2}{iq + \epsilon_p + \epsilon_k} \right] [f(-\epsilon_p) - f(\epsilon_k)], \tag{A2}
\end{aligned}$$

$$\begin{aligned}
L_{FF}(q, \mathbf{p}) &= T \sum_{ip} F(ip, \mathbf{p}) F^\dagger(ip + iq, \mathbf{k}) \\
&= u_p u_k v_p v_k \left\{ \left[\frac{1}{iq + \epsilon_p - \epsilon_k} - \frac{1}{iq - \epsilon_p + \epsilon_k} \right] [f(\epsilon_p) - f(\epsilon_k)] \right. \\
&\quad \left. + \left[\frac{1}{iq + \epsilon_p + \epsilon_k} - \frac{1}{iq - \epsilon_p - \epsilon_k} \right] [f(-\epsilon_p) - f(\epsilon_k)] \right\}, \tag{A3}
\end{aligned}$$

$$\begin{aligned}
L_{G^\dagger G}(q, \mathbf{p}) &= T \sum_{ip} G^\dagger(ip, \mathbf{p}) G(ip + iq, \mathbf{k}) \\
&= - \left[\frac{u_k^2 v_p^2}{iq + \epsilon_p - \epsilon_k} - \frac{u_p^2 v_k^2}{iq - \epsilon_p + \epsilon_k} \right] [f(\epsilon_p) - f(\epsilon_k)] \\
&\quad - \left[\frac{u_p^2 u_k^2}{iq - \epsilon_p - \epsilon_k} - \frac{v_p^2 v_k^2}{iq + \epsilon_p + \epsilon_k} \right] [f(-\epsilon_p) - f(\epsilon_k)], \tag{A4}
\end{aligned}$$

$$\begin{aligned}
L_{FG^\dagger}(q, \mathbf{p}) &= T \sum_{ip} F(ip, \mathbf{p}) G^\dagger(ip + iq, \mathbf{k}) \\
&= u_p v_p \left[\frac{v_p^2}{iq + \epsilon_p - \epsilon_k} + \frac{u_k^2}{iq - \epsilon_p + \epsilon_k} \right] [f(\epsilon_p) - f(\epsilon_k)] \\
&\quad - u_p v_p \left[\frac{v_k^2}{iq - \epsilon_p - \epsilon_k} - \frac{u_k^2}{iq + \epsilon_p + \epsilon_k} \right] [f(-\epsilon_p) - f(\epsilon_k)].
\end{aligned} \tag{A5}$$

The remainder loop integrals are obtained from those defined above through the relations

$$L_{G^\dagger G^\dagger}(iq, \mathbf{p}) = L_{GG}(-iq, \mathbf{p}), \quad L_{GF}(iq, \mathbf{p}) = L_{FG}(-iq, \mathbf{p}), \tag{A6}$$

$$L_{GG^\dagger}(iq, \mathbf{p}) = L_{G^\dagger G}(-iq, \mathbf{p}), \quad L_{G^\dagger F}(iq, \mathbf{p}) = L_{FG^\dagger}(-iq, \mathbf{p}), \tag{A7}$$

where, except for the first relation, we used the fact that the quasiparticle spectrum is reflection invariant, $\epsilon(-\mathbf{p}) = \epsilon(\mathbf{p})$. This means that we can interchange simultaneously $\mathbf{k} \leftrightarrow \mathbf{p}$ without affecting the result. The retarded polarization tensor is obtained by analytical continuation in the loop integrals $L_{X, X'}(iq, \mathbf{p}) = L_{X, X'}(\omega + i\delta, \mathbf{p})$ and by subsequent integration over the three-momentum \mathbf{p} according to the Eq. (31).

Next we concentrate on the pair-breaking contributions. The imaginary part of the associated polarization tensor can be written in the general form

$$\begin{aligned}
\Im \Pi_{XX'} &= -\pi \int \frac{d^3 p}{(2\pi)^3} K_{XX'}(u_p, v_p, u_k, v_k) \delta(\omega - \epsilon_p - \epsilon_k) [1 - f(\epsilon_p) - f(\epsilon_k)] \\
&\simeq -2\pi\nu(p_F) K_{XX'}(\mathbf{q} \rightarrow 0, \omega = 2\epsilon_p) \frac{\theta(\omega - 2\Delta)}{\sqrt{\omega^2 - 4\Delta^2}} \left[1 - 2f\left(\frac{\omega}{2}\right) \right],
\end{aligned} \tag{A8}$$

where $X, X' \in G, G^\dagger, F$. The kernels $K_{XX'}$ are deduced from the corresponding loop integrals above,

$$K_{GG} = u_k^2 v_p^2, \quad K_{FG} = u_p v_p u_k^2, \tag{A9}$$

$$K_{GF} = -u_k v_k v_p^2, \quad K_{FF} = -u_p v_p u_k v_k, \tag{A10}$$

$$K_{G^\dagger G} = -u_p^2 u_k^2 - 1, \quad K_{GG^\dagger} = -v_p^2 v_k^2, \tag{A11}$$

$$K_{FG^\dagger} = -u_p v_p v_k^2, \quad K_{G^\dagger F} = u_p^2 u_k v_k, \tag{A12}$$

$$K_{G^\dagger G^\dagger} = u_p^2 v_k^2. \tag{A13}$$

In the limit $\mathbf{q} \rightarrow 0$ and to the leading order in the parameter v_F^2/c^2

$$\left. \begin{array}{l} u^2 \\ v^2 \end{array} \right\} = \frac{1}{2} \left(1 \pm \frac{\sqrt{\omega^2 - 4\Delta^2}}{\omega} \right), \quad uv = \frac{\Delta}{\omega}. \tag{A14}$$

Since $K_{GG} = K_{G^\dagger G^\dagger}$, $K_{GF} = K_{FG^\dagger}$, and $K_{FG} = K_{G^\dagger F}$ there are six independent polarization tensors left. The real parts of the loop integrals and polarization tensors can be computed either through principal value integration in Eq. (A1)-(A5) or from their imaginary parts by making use of the Kramers-Kronig relation

$$\text{Re } \Pi_{XX'}(\omega) = \int \frac{d\omega'}{\pi} \frac{\Im \Pi_{XX'}(\omega')}{\omega' - \omega}. \tag{A15}$$

- [1] E. G. Flowers, M. Ruderman, and P. G. Sutherland, *Astrophys. J.* **205**, 541 (1976).
[2] D. N. Voskresensky and A. V. Senatorov, *Sov. J. Nucl. Phys.* **45**, 411 (1987) [*Yad. Fiz.* **45**, 657 (1987)].
[3] A. B. Migdal, E. E. Saperstein, M. A. Troitsky, and D. N. Voskresensky, *Phys. Rep.* **192**, 179 (1990).

- [4] Ch. Schaab, D. N. Voskresensky, A. Sedrakian, F. Weber, and M. K. Weigel, *Astron. Astrophys.* **321**, 591 (1996).
[5] S. Tsuruta, M. A. Teter, T. Takatsuka, T. Tatsumi, and R. Tamagaki, *Astrophys. J.* **571**, L143 (2002).
[6] D. Blaschke, H. Grigorian, and D. N. Voskresensky, *Astron. Astrophys.* **424**, 979 (2004).

- [7] D. Page, J. M. Lattimer, M. Prakash, and A. W. Steiner, *Astrophys. J. Suppl.* **155**, 2 (2004).
- [8] H. Grigorian and D. N. Voskresensky, *Astron. Astrophys.* **444**, 913 (2005).
- [9] V. A. Khodel, J. W. Clark, M. Takano, and M. V. Zverev, *Phys. Rev. Lett.* **93**, 151101 (2004).
- [10] D. N. Voskresensky, *Lecture Notes in Physics* vol. **578** (Springer-Verlag, New York, 2001) pg. 467.
- [11] A. Sedrakian, *Prog. Part. Nucl. Phys.* **58**, 168 (2007), eprint nucl-th/0601086.
- [12] D. G. Yakovlev, A. D. Kaminker, and K. P. Levenfish, *Astron. Astrophys.* **343**, 650 (1999).
- [13] A. D. Kaminker, P. Haensel, and D. G. Yakovlev, *Astron. Astrophys.* **345**, L14 (1999).
- [14] L. B. Leinson, *Nucl. Phys. A* **687**, 489 (2001).
- [15] A. Leggett, *Phys. Rev.* **147**, 119 (1966).
- [16] A. B. Migdal, *Theory of Finite Fermi Systems and Applications to Atomic Nuclei* (Interscience, London, 1967).
- [17] J. R. Schrieffer, *Theory of Superconductivity* (Benjamin, New York, 1964).
- [18] L. B. Leinson and A. Pérez, *Phys. Lett. B* **638**, 114 (2006).
- [19] D. Pines and C. Pethick, in *Proc. XIth Intern. Conf. on Low temperature physics*, ed. E. Kandu, (Kligatu Publ. Co., Tokyo, 1971).
- [20] J. W. Clark, C. G. Källman, C. H. Yang, and D. A. Chakkalakal, *Phys. Lett. B* **61**, 331 (1976).
- [21] J. M. C. Chen, J. W. Clark, E. Krotscheck, and R. A. Smith, *Nucl. Phys. A* **451**, 509 (1986).
- [22] J. M. C. Chen, J. W. Clark, R. D. Davé, and V. V. Khodel, *Nucl. Phys. A* **555**, 59 (1993).
- [23] J. Wambach, T. L. Ainsworth, and D. Pines, *Nucl. Phys. A* **555**, 128 (1993).
- [24] H.-J. Schulze, J. Cugnon, A. Lejune, M. Baldo, and U. Lombardo, *Phys. Lett. B* **375**, 1 (1996).
- [25] A. Schwenk, B. Friman, and G. Brown, *Nucl. Phys. A* **713**, 191 (2003).
- [26] A. Fabrocini, S. Fantoni, A. Y. Illarionov, and K. E. Schmidt, *Phys. Rev. Lett.* **95**, 192501 (2005).
- [27] C. Shen, U. Lombardo, P. Schuck, W. Zuo, and N. Sandulescu, *Phys. Rev. C* **67**, 061302(R) (2003).
- [28] A. Sedrakian, *Phys. Rev. C* **68**, 065805 (2003).
- [29] C. Shen, U. Lombardo, and P. Schuck, *Phys. Rev. C* **71**, 054301 (2005).
- [30] H. Müther and W. H. Dickhoff, *Phys. Rev. C* **72**, 054313 (2005).
- [31] U. Lombardo and H.-J. Schulze, *Lecture Notes in Physics* vol. **578** (Springer-Verlag, New York, 2001) pg. 30.
- [32] D. J. Dean and M. Hjorth-Jensen, *Rev. Mod. Phys.* **75**, 607 (2003).
- [33] A. Sedrakian and J. W. Clark, *Pairing in Fermionic Systems: Basic Concepts and Modern Applications*, (World Scientific, Singapore, 2007), in press, Chapt. 6.
- [34] A. A. Abrikosov, L. P. Gorkov, and I. E. Dzyaloshinski, *Methods of quantum field theory in statistical physics*, (Dover, New York, 1975).
- [35] R. Machleidt, *Phys. Rev. C* **63**, 024001 (2001).
- [36] W. H. Dickhoff, A. Faessler, J. Meyer-ter-Vehn, and H. Müther, *Phys. Rev. C* **23**, 1154 (1981).
- [37] A. Sedrakian and J. W. Clark, *Phys. Rev. C* **73**, 035803 (2006).
- [38] A. Sedrakian and A. E. L. Dieperink, *Phys. Lett. B* **463**, 145 (1999); *Phys. Rev. D* **62**, 083002 (2000).
- [39] U. Lombardo, P. Schuck, and W. Zuo, *Phys. Rev. C* **64**, 021301(R) (2001).
- [40] A. Sedrakian, T. T. S. Kuo, H. Müther, and P. Schuck, *Phys. Lett. B* **576**, 68 (2003).
- [41] J. Kucei, F. Montani, H. Müther, and A. Sedrakian, *Nucl. Phys. A* **723**, 32 (2003).
- [42] A. Sedrakian and U. Lombardo, *Phys. Rev. Lett.* **84**, 602 (2000).
- [43] U. Lombardo, P. Nozières, P. Schuck, H.-J. Schulze, and A. Sedrakian, *Phys. Rev. C* **64**, 064314 (2001).
- [44] A. Sedrakian, *Phys. Lett. B* **607**, (2005) 27.
- [45] P. Jaikumar, C. D. Roberts and A. Sedrakian, *Phys. Rev. C* **73**, 042801(R) (2006).
- [46] Q. Wang, eprint hep-ph/0607096.
- [47] Q. Wang, Z. G. Wang, and J. Wu, *Phys. Rev. D* **74**, 014021 (2006).
- [48] A. Schmitt, I. A. Shovkovy and Q. Wang, *Phys. Rev. D* **73**, 034012 (2006).
- [49] M. G. Alford and A. Schmitt, eprint nucl-th/0608019.
- [50] B. A. Sa 'd, I. A. Shovkovy, and D. H. Rischke, eprint astro-ph/0607643.
- [51] R. Anglani, G. Nardulli, M. Ruggieri, and M. Mannarelli, *Phys. Rev. D* **74**, 074005 (2006).
- [52] R. Anglani, eprint hep-ph 0610404.